Doubly Asymptotic Open Boundary Condition for Vector Wave Propagation in Semi-Infinite Layer

Suriyon Prempramote[1]

[1] **School of Civil and Environmental Engineering, The University of New South Wales, Sydney, NSW 2052, Australia**

E-mail: [1] s.prempramote@unswalumni.com

Abstract

The propagation of vector waves in a semi-infinite layer with a constant depth is addressed by extending the SBFEM. The extra coefficient matrix [E^1] appears in the SBFE equation. The doubly asymptotic continued fraction solution is derived to include the contribution of such a matrix. The factor matrices are introduced to the solution to improve the numerical stability of the solution. The coefficients of the solution are determined recursively by satisfying the SBFE equation in dynamic stiffness at both high- and low-frequency limits. By introducing auxiliary variables and using the doubly asymptotic continued fraction solution, the force — displacement relationship on the boundary is formulated as a high-order doubly asymptotic open boundary condition in the frequency domain, and a system of first-order ordinary differential equations in the time domain to which standard time-stepping schemes can be directly applied. No parameters other than the continued-fraction orders are selected by the user to increase the accuracy.

Keywords: wave propagation, open boundary condition, semi-infinite layer, SBFEM

1. Introduction

It is necessary to introduce an artificial boundary to the boundary of the computational domain whenever an unbounded domain is modeled for a wave propagation problem. The boundary condition enforced on such a boundary is aimed at absorbing propagating waves to prevent fictitious reflections at the boundary which often pollute the solution. Today there are several absorbing boundary conditions (ABCs) which can be classified into two groups. The ABCs in the first group are global and obtained from employing rigorous methods. In contrast, the ABCs in the second group are local and obtained from employing approximate methods. The global ABCs usually provide high accuracy and robustness, but are computationally expensive due to convolution integrals, while the local ones are geometrically universal, computationally efficient, but less accurate [1].

In the case of a long-time analysis of large-scale problems, the global ABCs are more impractical due to their large demand on storage capacity and computational time. This led to the search for high quality approximations that are spatially and temporally local [2]. Hence, a large number of local ABCs, for example the viscous boundary condition [3], were developed. To improve the accuracy of the boundary conditions, several high-order ABCs were thereafter proposed such as the BGT boundary condition [4], etc. Even though the high-order ABCs can increase the accuracy by increasing the order, they encounter difficulties in numerical implementation when the order is higher than two. In recent years, local high-order ABCs which are practically implementable for an arbitrary order, for example the Hagstrom-Warbutron ABC [5], have been proposed.

For vector wave propagation problems, most of existing high-order ABCs are singly asymptotic at high-frequency limit, specifically developed for circular and spherical boundaries. In the case of semi-infinite layers, a few ABCs are reported in literature, such as the high-order ABC developed by Guddati and Tassoulas [6]. Therefore, the open boundary condition developed herein is aimed at specifically applying to semi-infinite layers in both high- and low-frequency limits. The boundary condition is derived by extending the scaled boundary finite element method (SBFEM) [7] with use of the continued fraction technique.

2. Derivation of Doubly Asymptotic Open Boundary Condition

2.1 SBFE Equations

A semi-infinite layer with the mass density (ρ), Young's modulus (E), Poisson's ratio (ν) and a constant depth (h) is illustrated in Fig. 1. The layer is assumed to be isotropic, homogeneous and elastic. The in-plane motion (u=u(x,y,t) in the x-direction and v=v(x,y,t) in the y-direction) and the plane strain condition are considered.

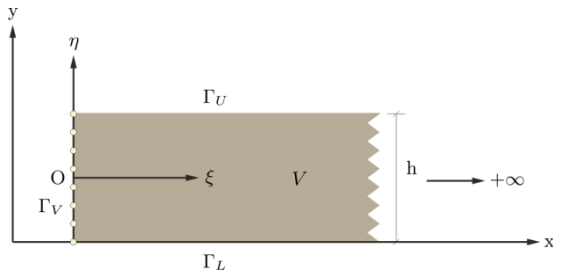

Fig. 1 Semi-Infinite Layer

For the boundary conditions, the vertical boundary Γ_V (at $x=x_b$) is subjected to time-dependent in-plane normal and shear stresses. Free condition is imposed on the upper boundary Γ_U and fixed condition on the lower boundary Γ_L. The governing equation of the layer in 2-D Cartesian coordinate can be expressed as

$$(\lambda+G)\phi_{,x}+G\nabla^2 u=\rho\ddot{u} \tag{1}$$

$$(\lambda+G)\phi_{,y}+G\nabla^2 v=\rho\ddot{v} \tag{2}$$

where the Laplace operator ∇^2, potential ϕ, Lamé constant λ and shear modulus G are defined as the following equations:

$$\nabla^2=\partial^2/\partial x^2+\partial^2/\partial y^2 \tag{3}$$

$$\phi=\varepsilon_x+\varepsilon_y \tag{4}$$

$$\lambda=E\nu/[(1+\nu)(1-2\nu)] \tag{5}$$

$$G=E/[2(1+\nu)] \tag{6}$$

For the coordinate transformation, it is expressed as

$$x(\xi)=x_b+\xi \tag{7}$$

$$y(\xi,\eta)=[N(\eta)]\{y_b\} \tag{8}$$

where $\{y_b\}$ is the scaled boundary coordinate vector.

By transforming Eqs. 1 and 2 to 3 and 4, using the Galerkin's weighted residual method on Γ_V, the SBFE equation in displacement in the frequency domain is subsequently formulated as

$$[E^0]\{W(\xi)\}_{,\xi\xi}+([E^1]^T-[E^1])\{W(\xi)\}_{,\xi}-[E^2]\{W(\xi)\}+\omega^2[M^0]\{W(\xi)\}=0 \tag{9}$$

where $[E^0]$, $[E^1]$, $[E^2]$ and $[M^0]$ are the coefficient matrices obtained by assembling all element coefficient matrices similar to those in the FEM, and $\{W(\xi)\}$ is the nodal displacement amplitude. The amplitude of the internal forces is in the form

$$\{Q(\xi)\}=[E^0]\{W(\xi)\}_{,\xi} \tag{10}$$

, which is related to the dynamic stiffness matrix $[S^\infty(\omega)]$ as

$$-\{Q(\xi)\}=[S^\infty(\omega)]\{W(\xi)\} \tag{11}$$

By eliminating $\{W(\xi)\}$ terms in Eq. 9 using Eqs. 10 and 11, the SBFE equation in dynamic stiffness is obtained as

$$([S^\infty(\omega)]+[E^1])[E^0]^{-1}([S^\infty(\omega)]+[E^1]^T)-[E^2]+\omega^2[M^0]=0 \tag{12}$$

2.2 Continued Fraction Solution

The solution in Eq. 12, $[S^\infty(\omega)]$ can be approximated as a continued fraction solution at the high-frequency limit ($\omega\to\infty$) as expressed in the following equation:

$$[S^\infty(\omega)]=[K_\infty]+(i\omega)[C_\infty]-[\psi^{(1)}][Y^{(1)}(\omega)]^{-1}[\psi^{(1)}]^T \tag{13}$$

$$[Y^{(i)}(\omega)]=[Y_0^{(i)}]+(i\omega)[Y_1^{(i)}]-[\psi^{(i+1)}][Y^{(i+1)}(\omega)]^{-1}[\psi^{(i+1)}]^T \quad (i=1,\ 2,\ \ldots,\ M_H) \tag{14}$$

where $[K_\infty]$, $[C_\infty]$, $[Y_0^{(i)}]$ and $[Y_1^{(i)}]$ are coefficient matrices to be determined recursively in the solution procedure. The factor matrices $[\psi^{(1)}]$ and $[\psi^{(i+1)}]$ are introduced to improve numerical stability of the solution. $[Y^{(M_H+1)}(\omega)]$ the residual in Eq. 14 is rewritten as $[Y_L(\omega)]$, which is solved at the low-frequency limit ($\omega\to0$),

$$[Y_L(\omega)]=[Y_{L0}^{(0)}]+(i\omega)[Y_{L1}^{(0)}]-(i\omega)^2[\psi_L^{(1)}][Y_L^{(1)}(\omega)]^{-1}[\psi_L^{(1)}]^T \tag{15}$$

$$[Y_L^{(i)}(\omega)]=[Y_{L0}^{(i)}]+(i\omega)[Y_{L1}^{(i)}]-(i\omega)^2[\psi_L^{(i+1)}][Y_L^{(i+1)}(\omega)]^{-1}[\psi_L^{(i+1)}]^T \quad (i=1,\ 2,\ \ldots,\ M_L) \tag{16}$$

where $[Y_{L0}^{(0)}]$, $[Y_{L1}^{(0)}]$, $[Y_{L0}^{(i)}]$ and $[Y_{L1}^{(i)}]$ are coefficient matrices to be determined recursively in the solution procedure. The factor matrices $[\psi_L^{(1)}]$ and $[\psi_L^{(i+1)}]$ are introduced to improve numerical stability of the solution.

2.3 Open Boundary Condition

By using the force $\{R\}$ – displacement $\{W\}$ relationship in the frequency domain

$$\{R\}=[S^\infty(\omega)]\{W\} \tag{17}$$

on Γ_V with the introduction of auxiliary variables i.e. $\{W^{(1)}\}$, $\{W^{(2)}\}$, etc. that are rewritten in terms of

$$[\psi^{(i+1)}]^T\{W^{(i)}\}=[Y^{(i+1)}(\omega)]\{W^{(i+1)}\} \quad (i=0,\ 1,\ \ldots,\ M_H) \tag{18}$$

at the high-frequency limit where $\{W^{(0)}\}=\{W\}$, and

$$(i\omega)[\psi_L^{(i+1)}]^T\{W_L^{(i)}\} = [Y_L^{(i+1)}(\omega)]\{W_L^{(i+1)}\} \quad (i=0,\ 1,\ \ldots,\ M_L) \tag{19}$$

at the low-frequency one where $\{W_L^{(0)}\}=\{W^{(M_H+1)}\}$, the open boundary condition enforced on Γ_V can be finally obtained in the time domain as

$$[K_h]\{z(t)\}+[C_h]\{\dot{z}(t)\}=\{f(t)\} \tag{20}$$

, which can be solved by employing standard time-stepping schemes e.g. Newmark's method, where

$$\{z(t)\}=[\{w\},\ \{\tilde{w}^{(1)}\},\ \ldots,\ \{\tilde{w}^{(M_H)}\},\ \{\tilde{w}_L^{(0)}\},\ \{\tilde{w}_L^{(1)}\},\ \ldots,\{\tilde{w}_L^{(M_L)}\}]^T \tag{21}$$

$$\{f(t)\}=[\{r\},\ 0,\ \ldots,\ 0,\ 0,\ 0,\ \ldots,\ 0]^T \tag{22}$$

$$[K_h]=\begin{bmatrix} [K_\infty] & -[\psi^{(1)}] & & & & & & & \\ -[\psi^{(1)}]^T & [Y_0^{(1)}] & -[\psi^{(2)}] & & & & & & \\ & -[\psi^{(2)}]^T & \ddots & \ddots & & & & & \\ & & \ddots & [Y_0^{(M_H)}] & -[\psi_L^{(0)}] & & & & \\ & & & -[\psi_L^{(0)}]^T & [Y_{L0}^{(0)}] & 0 & & & \\ & & & & 0 & [Y_{L0}^{(1)}] & \ddots & & \\ & & & & & \ddots & \ddots & 0 & \\ & & & & & & 0 & [Y_{L0}^{(M_L)}] \end{bmatrix} \tag{23}$$

$$[C_h]=\begin{bmatrix} [C_\infty] & 0 & & & & & & & \\ 0 & [Y_1^{(1)}] & 0 & & & & & & \\ & 0 & \ddots & \ddots & & & & & \\ & & \ddots & [Y_1^{(M_H)}] & 0 & & & & \\ & & & 0 & [Y_{L1}^{(0)}] & -[\psi_L^{(1)}] & & & \\ & & & & -[\psi_L^{(1)}]^T & [Y_{L1}^{(1)}] & \ddots & & \\ & & & & & \ddots & \ddots & -[\psi_L^{(M_L)}] & \\ & & & & & & -[\psi_L^{(M_L)}]^T & [Y_{L1}^{(M_L)}] \end{bmatrix} \tag{24}$$

3. Numerical Examples

The semi-infinite layer in Fig. 1 with the ratio of $G/\rho=1$, $\nu=0.25$ is tested in the following examples. The meshes of SBFEM and FEM are generated in Figs. 2(a) and 2(b), respectively.

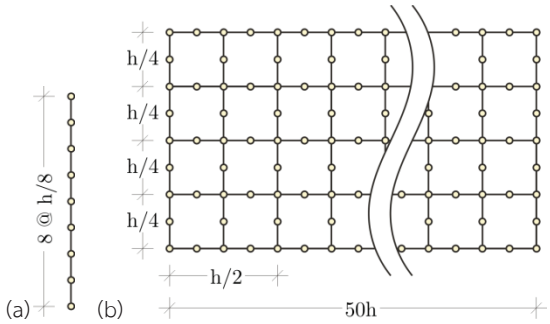

Fig. 2 Meshes: (a) SBFEM and (b) FEM

In the frequency-domain analysis, the solutions obtained from Eq. 13 (including Eqs. 14 to 16) are compared with the reference solutions obtained from Eq. 12. For convenience, the solutions are all plotted in terms of equivalent dynamic stiffness which is expressed as

$$S(\omega) = \{\varphi\}^T\left[S^\infty(\omega)\right]\{\varphi\} \tag{25}$$

where $\{\varphi\}$ denotes the linear spatial motion pattern of the nodes on Γ_V that does not vary with time [8] with respect to the dimensionless frequency ($a_0=\omega h/c_s$).

As plotted in Figs. 4 and 5, the accuracy of the solution increases when the orders M_H and M_L increase from 4 to 8 (see the red lines that almost fit the reference ones).

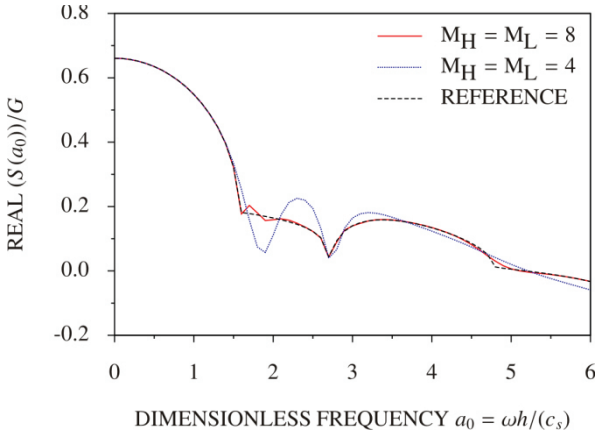

Fig. 3 Real Part of $S(\omega)$

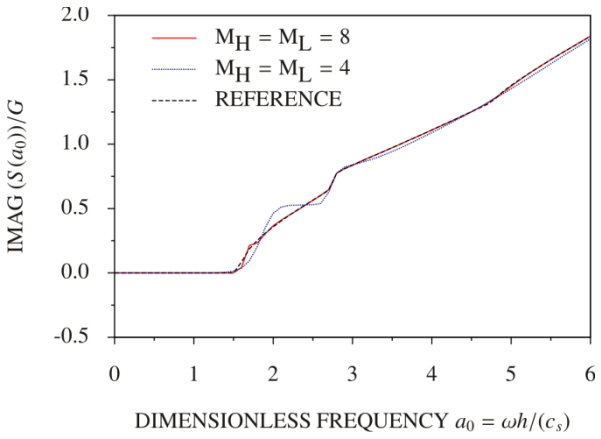

Fig. 4 Imaginary Part of $S(\omega)$

In the time-domain analysis, the Newmark's method with $\gamma=0.5$ and $\beta=0.25$ is adopted. An extended mesh analyzed by using ABAQUS is used as a reference solution to verify the open boundary condition. The displacement responses at Point A at the top of Γ_V are plotted with

respect to the dimensionless time ($\bar{t}$ =tc_s/h) to evaluate the accuracy of the open boundary condition.

3.1 Example 1

The semi-infinite layer is subjected to a surface traction p(t) in the x-direction (see Fig. 5) which is prescribed as a triangular function in Fig. 6. The maximum surface traction is denoted by P_T.

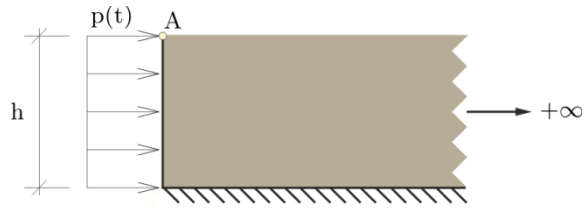

Fig. 5 Horizontal Surface Traction

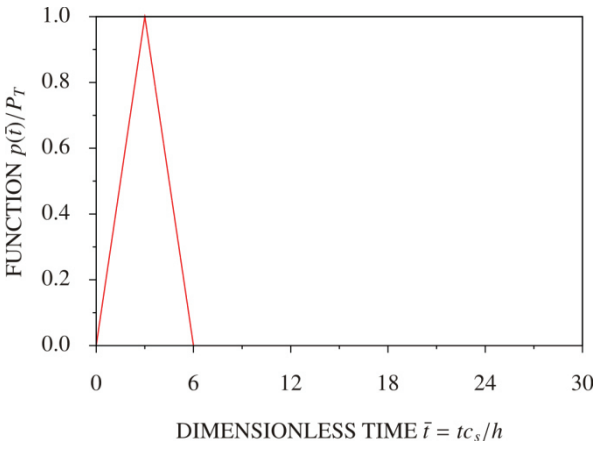

Fig. 6 Impulse

At the orders M_H=M_L=4, the horizontal and vertical displacements correspond to those of the extended mesh at only the early time as plotted in Figs. 7 and 8. As the orders increase to 8, the accuracy of all displacements at the late time is obviously improved (see the red lines).

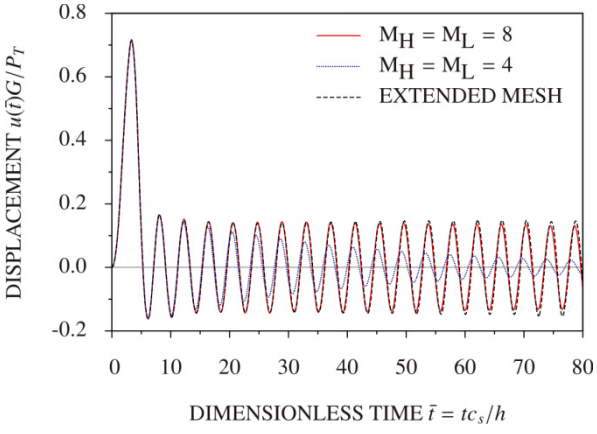

Fig. 7 Horizontal Displacement

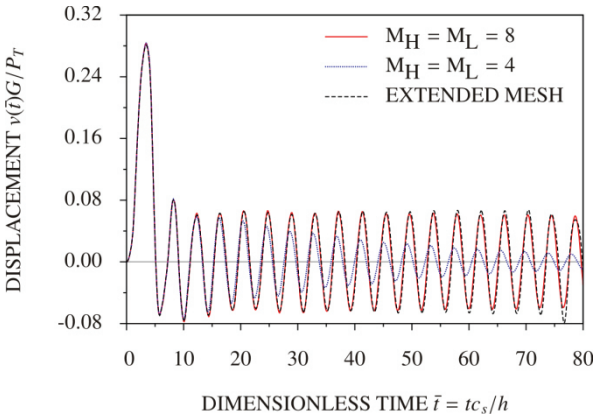

Fig. 8 Vertical Displacement

3.2 Example 2

The same uniform surface traction p(t) as in the first example is applied to this example but in the y-direction as illustrated in Fig. 9.

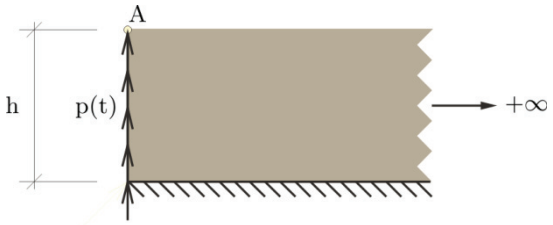

Fig. 9 Vertical Surface Traction

Similarly, the open boundary condition with M_H=M_L=4 is still tested first. All the displacements still correspond to those of the extended mesh at the early time as plotted in Figs. 10 and 11. Similarly, when the orders increase to 8, the accuracy of all displacements at the late time is improved.

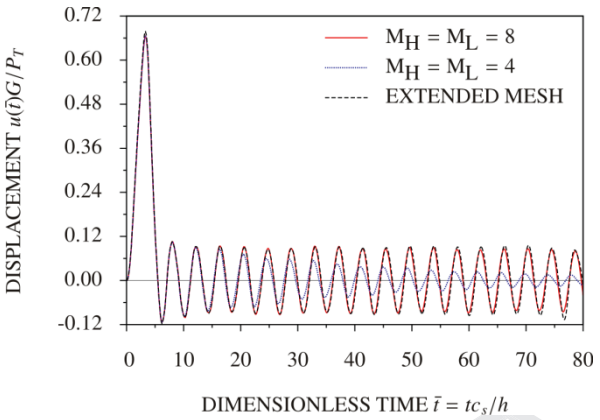

Fig. 10 Horizontal Displacement

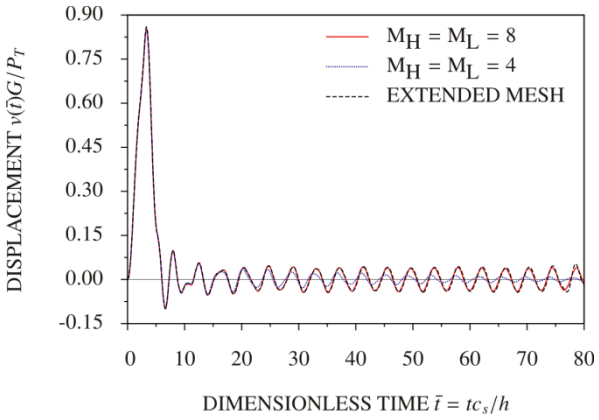

Fig. 11 Vertical Displacement

3.3 Example 3

In the last example, an inclined surface traction is applied to the semi-infinite layer as illustrated in Fig. 12. A Ricker wavelet in Fig. 13 is chosen as such a surface traction.

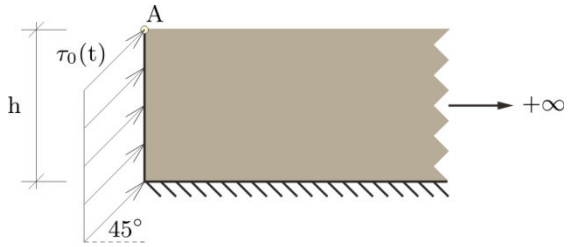

Fig. 12 Inclined Surface Traction

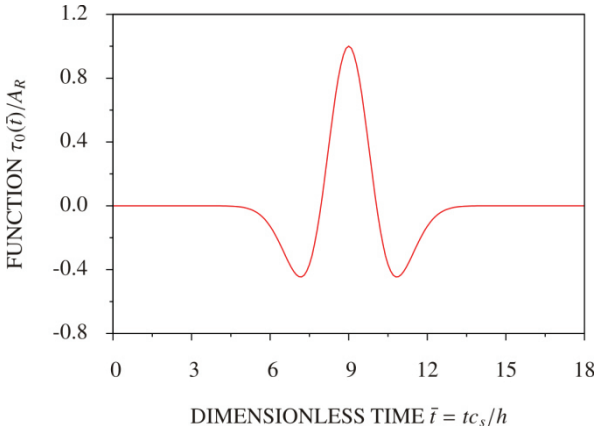

Fig. 13 Ricker Wavelet

The open boundary condition also yields the accurate displacements at the early time when the orders are equal to 4 for this type of surface traction. When the orders increase to 8, all the displacements are also improved at the late time as plotted in Figs. 14 and 15.

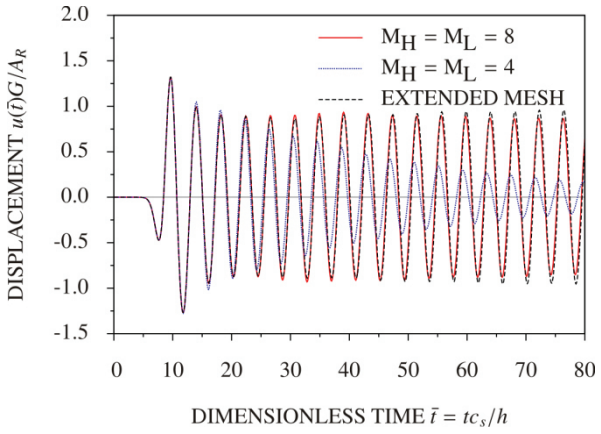

Fig. 14 Horizontal Displacement

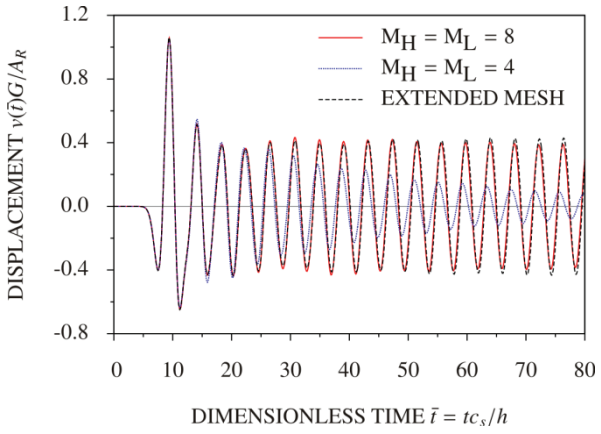

Fig. 15 Vertical Displacement

4. Conclusion

In the frequency-domain analysis, the solution obtained from the continued fractions converges the reference solution rapidly as the continued-fraction orders increase. No numerical stability problems are observed. In the time-domain analysis, the doubly asymptotic open boundary condition can yield the satisfied results. The displacement responses in both x- and y-directions correspond to those of the extended mesh method. No fictitious reflections are observed either.

5. Acknowledgement

I would like to express my gratitude to my supervisor, Professor Chongmin Song for his advice on this research.

References

[1] S. V. Tsynkov. “Numerical solution of problems on unbounded domains. A review”. *Applied Numerical Mathematics*, 27(4), pp. 465-532, August. 1998.

[2] E. Kausel. “Local transmitting boundaries”. *Journal of Engineering Mechanics*, 114(6), pp. 1011-1027, June. 1988.

[3] J. Lysmer and R. L. Kuhlemeyer. “Finite dynamic model for infinite media”. *Journal of the Engineering Mechanics Division*, 95(4), pp. 859-877, August. 1969.

[4] A. Bayliss and E. Turkel. “Far field boundary conditions for compressible flows”. *Journal of Computational Physics*, 48(2), pp. 182-199, November. 1982.

[5] T. Hagstrom and T. Warburton. “A new auxiliary variable formulation of high-order local radiation boundary conditions: corner compatibility conditions and extensions to first-order systems”. *Wave Motion*, 39(4), pp. 327-338, April. 2004.

[6] M. N. Guddati and J. L. Tassoulas. “Space-time finite elements for the analysis of transient wave propagation in unbounded layered media”. *International Journal of Solids and Structures*, 36(31), pp. 4699-4723, November. 1999.

[7] J. P. Wolf. *The Scaled Boundary Finite Element Method*. John Wiley & Sons, 2003, pp. 1-361.

[8] J. P. Wolf and C. Song, *Finite-Element Modelling of Unbounded Media*. John Wiley & Sons, 1996, pp. 281-282.